Title	Charged-impurity-induced Majorana fermions in topological superconductors
Author(s)	Zhou, T; Li, XJ; Gao, Y; Wang, Z
Citation	Physical Review B, 2015, v. 91, article no. 014512
Issued Date	2015
URL	http://hdl.handle.net/10722/208261
Rights	Physical Review B. Copyright © American Physical Society.

Charged-impurity-induced Majorana fermions in topological superconductors

Tao Zhou* and Xiao-Jing Li
College of Science, Nanjing University of Aeronautics and Astronautics, Nanjing 210016, China

Yi Gao
Department of Physics and Institute of Theoretical Physics, Nanjing Normal University, Nanjing 210023, China

Z. D. Wang†
Department of Physics and Center of Theoretical and Computational Physics, The University of Hong Kong, Pokfulam Road, Hong Kong, China

(Received 20 October 2014; revised manuscript received 13 January 2015; published 26 January 2015)

We study numerically Majorana fermions (MFs) induced by a charged impurity in topological superconductors. It is revealed from the relevant Bogoliubov–de Gennes equations that (i) for quasi-one-dimensional systems, a pair of MFs are bounded at the two sides of one charged impurity and are well-separated; and (ii) for a two-dimensional square lattice, the charged-impurity-induced MFs are similar to the known pair of vortex-induced MFs, in which one MF is bounded by the impurity while the other appears at the boundary. Moreover, the corresponding local density of states is explored, demonstrating that the presence of MF states may be tested experimentally.

DOI: 10.1103/PhysRevB.91.014512 PACS number(s): 71.10.Pm, 03.67.Lx, 74.90.+n

I. INTRODUCTION

Topological superconductors have recently attracted a tremendous amount of attention due to their exotic properties and potential applications [1]. There are a number of candidate systems for realizing topological superconductors. One well-known example is the chiral $p+ip$ superconductor [2,3], although its experimental realization is a great challenge. A more realistic model may be the superconducting systems realized in the spin-orbital coupled s-wave, such as the $Cu_xBe_2Se_3$ material [4–7]. Besides, topological superconductors may also be fabricated in heterostructure systems, including a semiconductor with the spin-orbital interaction and a conventional s-wave superconductor [3,8–15]. Another promising candidate is topological superfluid, which may also be simulated by cold atom systems, noting that both s-wave pairing and spin-orbital coupling have been implemented in cold atoms [16–20].

As is known, one of the most prominent features of a topological superconductor lies in the fact that topologically nontrivial Majorana fermions (MFs) may emerge in the system, which is relevant to the non-Abelian statistics and has potential applications in topological quantum computation [21]. It was indicated that the MFs may exist in the vortex cores of a chiral $p+ip$ superconductor [2] and they should obey non-Abelian statistics [22]. Later there are a number of theoretical proposals for realizing and probing the MFs in various topological superconducting systems [23–33]. Although significant experimental efforts have been made on MFs [10–15,34], there is as of yet no unambiguous evidence for the MFs and no direct demonstration of their non-Abelian statistics.

On the other hand, the impurity effect has been an important issue in the study of unconventional superconductivity [35]. For a d-wave superconducting system, one remarkable result is the existence of the midgap bound state near the impurity site, while such a bound state does not exist for conventional s-wave superconductors. For a topological superconducting system, the existence of the midgap state is of great interest and may be related to the MF modes. Thus the impurity effect is also of interest, and it has attracted attention [36–42]. Contrary to the impurity effect of a topologically trivial s-wave superconductor, it has been reported that in-gap bound states may be induced by a nonmagnetic impurity [36–42]. The midgap state exists in a pure one-dimensional system [37] or in a two-dimensional system, but considering a typical line-type potential [38,39]. In general, however, for two- and three-dimensional systems, in-gap bound states appear at finite energy, and no zero-energy states exist near the impurity [38,40,41]. As a result, no MFs are actually induced by a single impurity for two- or three-dimensional system. Notably, previous studies on the single impurity effect have focused merely on the single neutral nonmagnetic in-plane impurity, in which the impurity term was treated theoretically as an additional potential on the impurity site. In contrast, we investigate here the effect of an off-plane charged impurity in a topological superconductor, with the impurity term being simulated by an additional Coulomb potential, noting that the charged-impurity effect has been studied intensively for some condensed-matter systems, such as high-T_c superconductors [43] and graphene layers [44]. More interestingly, we find that the charged-impurity effect is significantly different from that of the neutral nonmagnetic in-plane impurity, namely for a charged impurity, MFs indeed exist in the topological superconducting system. It is revealed that a pair of MFs are bounded by the charged impurity. As a result, one may manipulate the MFs by controlling the charged impurities, such that they may have potential applications in topological quantum computation.

This article is organized as follows. In Sec. II, we introduce the model and work out the formalism. In Sec. III, we perform

*tzhou@nuaa.edu.cn
†zwang@hku.hk

numerical calculations and discuss the obtained results. Finally, we give a brief summary in Sec. IV.

II. HAMILTONIAN AND FORMALISM

We start from a model Hamiltonian that includes the spin-orbital coupling, the Zeeman field, the s-wave pairing term, and an additional charged-impurity term, which is given by

$$H = H_t + H_\Delta + H_{\rm SO}, \tag{1}$$

where H_t includes the hopping term, the on-site potential, and the Zeeman field, expressed by

$$H_t = -t\sum_{\langle \mathbf{ij}\rangle}(c^\dagger_{\mathbf{i}\sigma}c_{\mathbf{j}\sigma} + \text{H.c.}) + \sum_{\mathbf{i}\sigma}(U_\mathbf{i} - \mu + \sigma h)c^\dagger_{\mathbf{i}\sigma}c_{\mathbf{i}\sigma}. \tag{2}$$

$\langle \mathbf{ij}\rangle$ represents the nearest-neighbor sites, h is the Zeeman field, and σ takes "+" for the spin-up state and "−" for the spin-down state. $U_\mathbf{i}$ is a site-dependent potential induced by the charged impurity. μ is the chemical potential.

H_Δ is the pairing term, expressed by

$$H_\Delta = \sum_\mathbf{i}(\Delta_\mathbf{ii}c^\dagger_{\mathbf{i}\uparrow}c^\dagger_{\mathbf{i}\downarrow} + \text{H.c.}), \tag{3}$$

and $H_{\rm SO}$ is the spin-orbital interaction, with

$$H_{\rm SO} = \sum_\mathbf{i}(i\lambda c^\dagger_{\mathbf{i}\uparrow}c_{\mathbf{i}+\hat{x}\downarrow} + i\lambda c^\dagger_{\mathbf{i}\downarrow}c_{\mathbf{i}+\hat{x}\uparrow} + \text{H.c.} + \lambda c^\dagger_{\mathbf{i}\uparrow}c_{\mathbf{i}+\hat{y}\downarrow} - \lambda c^\dagger_{\mathbf{i}\downarrow}c_{\mathbf{i}+\hat{y}\uparrow} + \text{H.c.}). \tag{4}$$

The above Hamiltonian can be diagonalized by solving the Bogoliubov–de Gennes (BdG) equations,

$$\sum_\mathbf{j}\begin{pmatrix} H_{\mathbf{ij}\uparrow\uparrow} & H_{\mathbf{ij}\uparrow\downarrow} & \Delta_\mathbf{jj} & 0 \\ H_{\mathbf{ij}\downarrow\uparrow} & H_{\mathbf{ij}\downarrow\downarrow} & 0 & -\Delta_\mathbf{jj} \\ \Delta^*_\mathbf{jj} & 0 & -H_{\mathbf{ij}\downarrow\downarrow} & -H^*_{\mathbf{ij}\downarrow\uparrow} \\ 0 & -\Delta^*_\mathbf{jj} & -H^*_{\mathbf{ij}\uparrow\downarrow} & -H_{\mathbf{ij}\uparrow\uparrow} \end{pmatrix}\Psi^\eta_\mathbf{j} = E_\eta\Psi^\eta_\mathbf{j}, \tag{5}$$

where $\Psi^\eta_\mathbf{j} = (u^\eta_{\mathbf{j}\uparrow}, u^\eta_{\mathbf{j}\downarrow}, v^\eta_{\mathbf{j}\downarrow}, v^\eta_{\mathbf{j}\uparrow})^{\rm T}$. $H_{\mathbf{ij}\sigma\sigma}$ and $H_{\mathbf{ij}\sigma\bar{\sigma}}$ $(\sigma \neq \bar{\sigma})$ are obtained from H_t and $H_{\rm SO}$, respectively. The site-dependent order parameter $\Delta_\mathbf{jj}$ is calculated self-consistently,

$$\Delta_\mathbf{jj} = \frac{V}{2}\sum_\eta u^\eta_{\mathbf{j}\uparrow}v^{\eta *}_{\mathbf{j}\downarrow}\tanh\left(\frac{E_\eta}{2K_BT}\right), \tag{6}$$

with V being the pairing strength.

The on-site particle number $n_\mathbf{i}$ is expressed as

$$n_\mathbf{i} = \sum_{\eta\sigma}\left|u^\eta_{\mathbf{i}\sigma}\right|^2 f(E_\eta), \tag{7}$$

with $f(E_\eta)$ the Fermi distribution function.

The local density of states (LDOS) can be calculated as

$$\rho_\mathbf{i}(\omega) = \sum_\eta\left[\left|u^\eta_{\mathbf{i}\uparrow}\right|^2\delta(E_\eta - \omega) + \left|v^\eta_{\mathbf{i}\downarrow}\right|^2\delta(E_\eta + \omega)\right], \tag{8}$$

where the delta function $\delta(E)$ is taken as $\delta = \Gamma/[\pi(E^2 + \Gamma^2)]$, with the quasiparticle damping $\Gamma = 0.01$.

In the present work, we consider an off-plane charged impurity carrying the negative electric charge $-Ze$, as sketched in Fig. 1. A repulsive potential $U_\mathbf{i} = U_0/\sqrt{(\mathbf{R_i} - \mathbf{r_0})^2 + (d/a)^2}$ is induced by the impurity, with $U_0 = Ze^2/(4\pi\varepsilon_0 a)$ (a is the lattice constant). In the following calculations, we set $Z = 1$ and $a = 4$ Å. U_0 is estimated to be about 3.6 eV. We use the hopping constant t to be the energy unit, and we set $U_0 = 6$. The distance d plays a key role in controlling the effective scope of the Coulomb potential. As d tends to zero, the potential at $\mathbf{r_0}$ approaches infinity. In this case, the charged impurity is equivalent to a unitary in-plane neutral nonmagnetic impurity [45]. As d increases, the long-range Coulomb interactions take effect. In the present work, we set $d = a$ for illustration. Generally, the MF modes are quite robust for larger U_0 and d. The numerical calculations are performed on the quasi-one-dimensional system with lattice size 400×3, and on the two-dimensional system with lattice size 48×48. Note that for both systems, we have verified numerically that no zero-energy state exists for a single-point-type nonmagnetic impurity (not presented here).

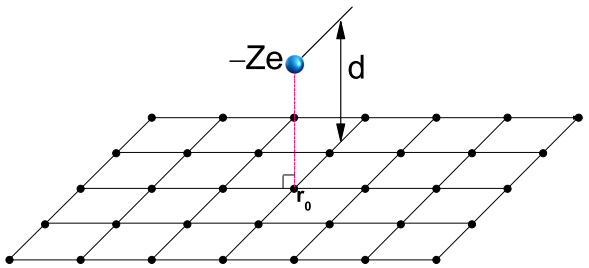

FIG. 1. (Color online) Schematic illustration of an off-plane charged impurity, with d being the distance between the plane and the impurity.

The other parameters and the corresponding phase diagram in the absence of impurity have already been discussed in some detail [46]. Here they are set as $\mu = -4$, $\lambda = 0.5$, $h = 0.6$, and $V = 5$, such that the system is in the topological superconducting phase. We have also checked numerically that our main results presented below are not sensitive to the parameters in the topological phase region. To see the origin of the topological feature more clearly, we transform the bare Hamiltonian into momentum space, with the two renormalized normal state energy bands, $E_\pm$, expressed as

$$E_\pm = \varepsilon_\mathbf{k} \pm \sqrt{h^2 + 4\lambda^2(\sin^2 k_x + \sin^2 k_y)}. \tag{9}$$

Here, $\varepsilon_\mathbf{k} = -2t(\cos k_x + \cos k_y) - \mu$. We plot the above band structure with $\mu = 0$ in Fig. 2. Since these two bands are both the superposition of the spin-up and spin-down electrons, with an additional s-wave pairing, the Hamiltonian is equivalent to a two-band $p \pm ip$-pairing superconducting system with opposite chirality, which is usually a topologically trivial superconductor. On the other hand, as is seen in Fig. 2, the two energy bands are separated by the Zeeman field with an energy gap $2h$ at the (0,0) point. If we set the chemical potential μ to be inside the gap (e.g., for the case of $\mu = -4$), then the upper band is unoccupied and only the lower band takes effect. In this case, the system is topologically nontrivial and equivalent to a one-band $p + ip$ superconducting system.

III. RESULTS AND DISCUSSION

We now present the numerical results for a quasi-one-dimensional system. The periodic boundary condition is

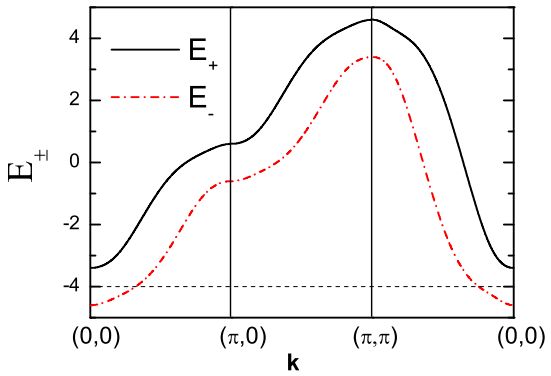

FIG. 2. (Color online) The renormalized normal state band dispersion in momentum space [Eq. (6)].

considered for both the x and y directions. For the quasi-one-dimensional lattice, the y dependence of the physical quantities is not important. Thus we just consider here the x dependence of the physical quantities, defined as $A(x) = 1/N_y \sum_y A(x,y)$. Figure 3(a) displays the self-consistent results of the superconducting gap and the site-dependent particle number. As is seen, both the superconducting gap and the on-site particle number are suppressed to zero near the impurity site. The energy gap increases and tends to be uniform away from the impurity. As a result, two gap edges at the sites $x = 200 \pm 10$ are induced by the charged impurity. This result is consistent with the energy band dispersion shown in Fig. 2 . As is seen, the minimum normal state energy is -4.6. Thus the particle number and the pairing gap will be suppressed to zero as $-\mu + U_{\mathbf{i}} > 4.6$, which yields the gap edges about 10 lattice sizes away from the impurity.

The existence of the gap edge is important for the MFs. We now demonstrate numerically the existence of the MF states. The information of the MFs can be obtained by diagonalizing the BdG equations [Eq. (2)]. The eigenvalues of the BdG Hamiltonian are plotted in Fig. 3(b). As is seen, two zero-energy eigenvalues are revealed by the numerical results. They are protected by an energy gap about 0.1. As is known, the two eigenvalues $\pm E$ come from one physical particle, expressed as C and $C^\dagger$, which are eigenvectors of the BdG Hamiltonian. For the case of $E = 0$, one physical particle can be separated as two MFs. The particle operators of the two MFs can be obtained by $\gamma_1 = (C + C^\dagger)/\sqrt{2}$ and $\gamma_2 = i(C^\dagger - C)/\sqrt{2}$. Then the spatial distribution of the MFs, $\gamma_{1,2}$, can be studied numerically. As is presented in Figs. 3(a) and 3(c), a pair of MFs are separated by the impurity and located near the two gap edges. This feature of well separated and localized MFs is rather important for the manipulation of them, which can be controlled by varying the position and scattering potential of the impurity, having potential applications in topological quantum computing [21].

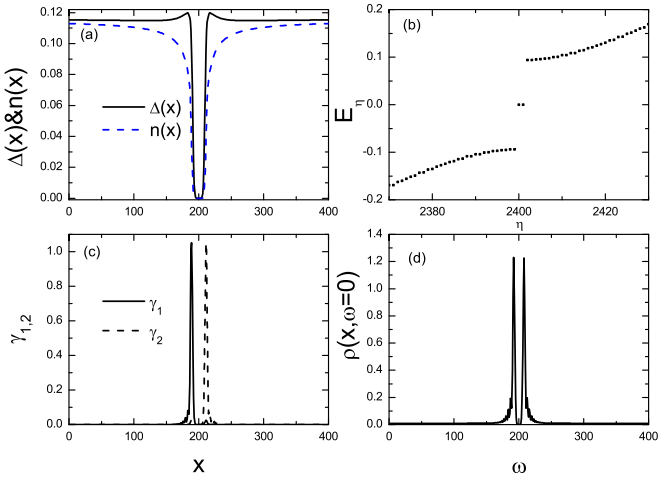

FIG. 3. (Color online) The numerical results for a 400×3 lattice. (a) The self-consistent results of the order parameter Δ and the site-dependent particle number n. (b) The eigenvalues of the Hamiltonian. (c) The spatial distributions of the two MFs. (d) The intensity plot of the LDOS at zero energy.

The existence of the zero mode can be examined through the LDOS spectra. The intensity of the zero-energy LDOS at different positions is plotted in Fig. 3(d). As is seen, there exists a sharp peak at the sites $x = 200 \pm 10$. It is clear that the zero-energy LDOS is qualitatively the same with the spatial distribution of the two MFs. The zero-bias peak of the LDOS can be tested by scanning tunneling microscope experiments. Thus the indication of MFs may be tested experimentally.

Let us turn to present the numerical results of a two-dimensional lattice with a charged impurity located at $\mathbf{r_0} = (24,24)$. The intensity plot of the order parameter magnitude and the on-site particle number with the open boundary condition are displayed in Figs. 4(a) and 4(b), respectively. Their two-dimensional cuts (along $y = 24$) are plotted in Fig. 4(c). As is seen, both the order-parameter magnitude and the particle number are near zero as $|\mathbf{R_i} - \mathbf{r_0}| < 10$. This result is similar to the case of a quasi-one-dimensional system and can be understood through the band structure shown in Fig. 2. As $|\mathbf{R_i} - \mathbf{r_0}| > 10$, the effective on-site potentials cross the

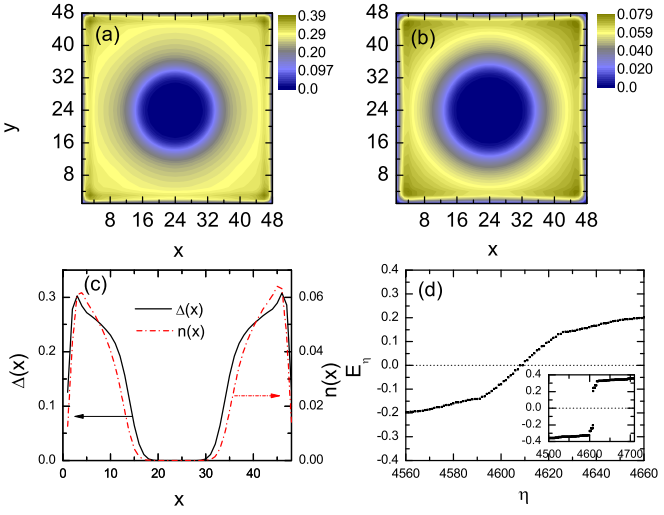

FIG. 4. (Color online) The numerical results for a 48×48 lattice. (a) The intensity plot of the order parameter. (b) The intensity plot of the site-dependent particle number. (c) The two-dimensional cuts of the order parameter and the particle number along $x = 24$. (d) The eigenvalues of the Hamiltonian in the presence of a charge-impurity. Inset of (d): The eigenvalues of the Hamiltonian with the periodic boundary and without the impurity.

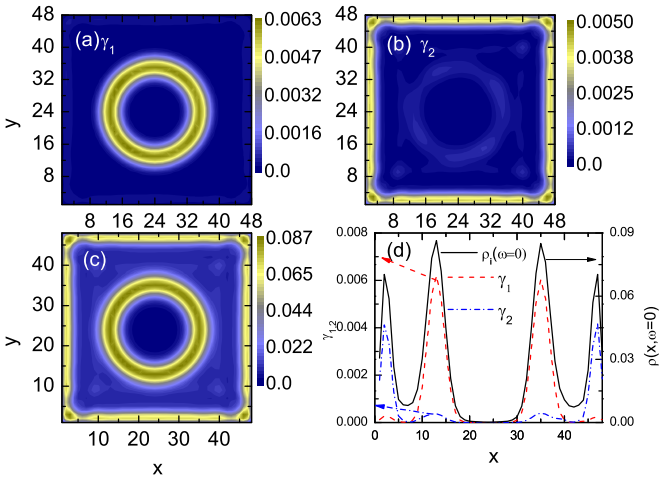

FIG. 5. (Color online) The numerical results for the 48×48 lattice. (a) The spatial distribution of γ_1. (b) The spatial distribution of γ_2. (c) The intensity plot of the zero-energy LDOS. (d) The two-dimensional cuts of panels (a)–(c) along $y = 24$.

lower energy band, and thus the on-site particle number and the gap magnitude increase. As a result, the gap edges at the sites $|\mathbf{R_i} - \mathbf{r_0}| = 10$ form. An edge state should exist and the MFs may exist near the gap edges. The eigenvalues of the two-dimensional Hamiltonian are plotted in Fig. 4(d). We also plot the eigenvalues for the case of the uniform pairing states with periodic boundary in the inset of Fig. 4(d). For the two-dimensional lattice in the presence of the boundaries, it is expected that an edge state crossing zero energy should exist. In the uniform superconducting state, an energy gap about 0.2 is seen clearly. In the presence of a charged impurity, as seen in Fig. 4(d), the edge state crossing the zero energy exists, protected by a bulk energy gap about 0.2. Two zero-energy eigenvalues can be seen clearly, related to the MF modes near the gap edges.

Similar to the case of the quasi-one-dimensional lattice, the two MFs can be studied numerically from the eigenvectors of the zero eigenvalues. The numerical results of the spatial distribution of the two MF states are presented in Figs. 5(a) and 5(b). We also plotted the zero-energy LDOS in Fig. 5(c) to disclose a possible experimental observation of the existence and distribution of the zero mode. Their two-dimensional cuts along the line $y = 24$ are plotted in Fig. 5(d).

As is shown in Figs. 5(a) and 5(b), the two well-separated MFs are identified numerically. The spatial distribution of γ_1 forms a circle with a radius of about 10 lattice sizes. Thus it appears near the superconductor-insulator boundary. Another MF γ_2 appears at the system boundary. These results are qualitatively the same as those in the case of the vortex-induced MFs in topological superconductors [2]. In this sense, here the charged impurity may be viewed as an artificially created vortex. One may manipulate the MFs through controlling the charged impurity. Similar to the case of the quasi-one-dimensional lattice, the zero mode can be detected experimentally through the zero-energy LDOS. The intensity plot of the zero-energy LDOS is displayed in Fig. 5(d). Here the spectrum is qualitatively consistent with the distributions of the two MF states. As a result, a signature of MFs may also be obtained through the LDOS spectra for the two-dimensional lattice system.

Experimentally, the LDOS spectra are measured via scanning tunneling spectroscopy. Several groups have recently reported a zero-bias peak in various systems [12–15], providing a possible indication of the existence of MFs, although it is still debatable. A number of theoretical proposals have been suggested so far [47–51]. However, detecting the MFs in a more direct way is rather challenging, and there has been no direct and convincing experimental evidence that confirms the existence of the MFs. We think that such evidence may be provided through probing the non-Abelian statistics of the quasiparticles. In the present work, the MFs are controllable in principle, and thus the exotic non-Abelian statistics may be demonstrated through coupling the system to a "quantum dot" [52]. In addition, if the position of the charged impurity is well-controlled, the braiding of the particles can be done directly, which may provide a promising method to detect and to confirm the existence of the MFs. Moreover, realization of the braiding may significantly promote applications of MFs in topological quantum computations in the near future.

It is also insightful to address the dependence of the above results on the parameters of the charged impurity. As seen in Fig. 4, there exists a charged-impurity-induced insulating "hole" with radius R_h around 10 lattice constants. Here the radius (R_h) is quite important for the appearance of a single MF. We have checked numerically this point for different sets of parameters (Z,d, and a). For example, only one MF appears in one hole for the range $6 \leqslant R_H \leqslant 20$, which gives $0.7 \leqslant Z \leqslant 2$ for the case of $d = a = 4$ Å, or $0.5 \leqslant Z \leqslant 1.5$ for $d = a = 3$ Å. Thus our main results seem to be robust against the parameters within a reasonable range, making it possible to realize the proposal with current experimental technology.

We now elaborate on the difference between charged-impurity-induced MFs and vortex-induced ones. As is known, the vortex is normally associated with a magnetic flux. The effect of the flux has been discussed in detail in Ref. [3], i.e., each vortex with magnetic flux binds a single zero-energy Majorana mode inside this vortex, regardless of the size of the vortex/flux [2,3]. However, when the magnetic flux is absent, the zero-energy state shifts to low-energy states. Therefore, the magnetic flux is important not only for creating the vortex, but also for the appearance of the Majorana mode itself in the vortex. On the other hand, in the present work, the excitations of MFs are mainly determined by the hole size created by the impurity. It is controlled by the parameters (a,Z, and d). The MF excitation emerges when a large insulating hole is induced. As the hole size decreases to be less than a critical radius R_c (about six lattice constants, as discussed above), the zero-energy state shifts to finite-energy states, and no MFs are excited in this case, which is consistent with previous studies on the pointlike impurity effect [38,40,41]. Also, the emergence of MFs in a rather extended parameter region is a noteworthy result. Further detailed studies on this issue will be of interest.

Finally, we would like to remark on the significance of the present work. First, we propose here an effective tool to realize MFs subject to an off-plane charged impurity. The MFs are bounded by the impurity. Technically they may be well controlled through operating the impurities. Secondly,

the two MFs are well separated in space, and there is almost no overlap. This is different from the case of the MF states induced by a harmonic potential [32]. Actually, the harmonic potential increases and tends to be infinite far away from the trapping center. Thus the superconducting region will only exist in a small region. Thus the two MFs subject to a harmonic potential are close in space. As a result, the two MFs should overlap in space. On the other hand, for the MFs induced by the Coulomb interaction, the potential tends to zero far away from the impurity center. For the large system size, the two MFs are sufficiently separated. This feature is of importance and may merit further application in topological quantum computation. Thirdly, for the two-dimensional lattice, the property of the MFs is qualitatively similar to that of the vortex-bounded MFs. Therefore, the non-Abelian statistics feature may be seen more easily in experiments as the charged impurities can be well-controlled, which is of fundamental interest. Finally, it is worthwhile pointing out that there exists another significant difference between the present work and the previous one on the MFs induced by a harmonic potential [32]. In Ref. [32], the numerical calculation is based on a typical model that considers a spin-dependent hopping term, which was proposed to be realized in cold atom systems. However, our numerical calculations and main results here are based on a standard model of topological superconductors. They may be generalized to other topological superconducting systems, e.g., the $p + ip$ superconducting systems or the semiconductor nanowire/s-wave superconductor heterostructure system.

IV. SUMMARY

In summary, we have studied numerically the effect of an off-plane charged impurity in topological superconductors. We have revealed that the MFs can be induced by the impurity. For a quasi-one-dimensional system, a pair of MFs are located at the two sides of the impurity, while for a two-dimensional system, one MF is bounded by the impurity and the other appears at the boundary of the system. The LDOS spectra have also been calculated, based upon which a clear indication of the MFs may be observed experimentally.

ACKNOWLEDGMENTS

This work was supported by the NSFC (Grants No. 11374005 and No. 11204138), the NCET (Grant No. NCET-12-0626), the NFRPC (Grant No. 2011CB922104), Jiangsu Qingnan engineering project, the GRF (Grants No. HKU7045/13P and No. HKU173051/14P), and the CRF (Grant No. HKU8/11G) of Hong Kong.

[1] X.-L. Qi and S.-C. Zhang, Rev. Mod. Phys. **83**, 1057 (2011).
[2] N. Read and D. Green, Phys. Rev. B **61**, 10267 (2000).
[3] J. Alicea, Rep. Prog. Phys. **75**, 076501 (2012).
[4] Y. S. Hor, A. J. Williams, J. G. Checkelsky, P. Roushan, J. Seo, Q. Xu, H. W. Zandbergen, A. Yazdani, N. P. Ong, and R. J. Cava, Phys. Rev. Lett. **104**, 057001 (2010).
[5] L. A. Wray, S.-Y. Xu, Y. Xia, Y. S. Hor, D. Qian, A. V. Fedorov, H. Lin, A. Bansil, R. J. Cava, and M. Zahid Hasan, Nat. Phys. **6**, 855 (2010).
[6] L. A. Wray, S. Xu, Y. Xia, D. Qian, A. V. Fedorov, H. Lin, A. Bansil, L. Fu, Y. S. Hor, R. J. Cava, and M. Z. Hasan, Phys. Rev. B **83**, 224516 (2011).
[7] S. Sasaki, M. Kriener, K. Segawa, K. Yada, Y. Tanaka, M. Sato, and Y. Ando, Phys. Rev. Lett. **107**, 217001 (2011).
[8] R. M. Lutchyn, J. D. Sau, and S. Das Sarma, Phys. Rev. Lett. **105**, 077001 (2010).
[9] Y. Oreg, G. Refael, and F. von Oppen, Phys. Rev. Lett. **105**, 177002 (2010).
[10] J. R. Williams, A. J. Bestwick, P. Gallagher, S. S. Hong, Y. Cui, A. S. Bleich, J. G. Analytis, I. R. Fisher, and D. Goldhaber-Gordon, Phys. Rev. Lett. **109**, 056803 (2012).
[11] L. P. Rokhinson, X. Liu, and J. K. Furdyna, Nat. Phys. **8**, 795 (2012).
[12] M. T. Deng, C. L. Yu, G. Y. Huang, M. Larsson, P. Caroff, and H. Q. Xu, Nano Lett. **12**, 6414 (2012).
[13] A. Das, Y. Ronen, Y. Most, Y. Oreg, M. Heiblum, and H. Shtrikman, Nat. Phys. **8**, 887 (2012).
[14] V. Mourik, K. Zuo, S. M. Frolov, S. R. Plissard, E. P. A. M. Bakkers, and L. P. Kouwenhoven, Science **336**, 1003 (2012).
[15] E. J. H. Lee, X. Jiang, M. Houzet, R. Aguado, C. M. Lieber, and S. De Franceschi, Nat. Nano. **9**, 79 (2014).
[16] T. Bourdel, L. Khaykovich, J. Cubizolles, J. Zhang, F. Chevy, M. Teichmann, L. Tarruell, S. J. J. M. F. Kokkelmans, and C. Salomon, Phys. Rev. Lett. **93**, 050401 (2004).
[17] J. K. Chin, D. E. Miller, Y. Liu, C. Stan, W. Setiawan, C. Sanner, K. Xu, and W. Ketterle, Nature (London) **443**, 961 (2006).
[18] Y.-J. Lin, K. Jimenez-Garcia, and I. B. Spielman, Nature (London) **471**, 83 (2011).
[19] P. Wang, Z.-Q. Yu, Z. Fu, J. Miao, L. Huang, S. Chai, H. Zhai, and J. Zhang, Phys. Rev. Lett. **109**, 095301 (2012).
[20] L. W. Cheuk, A. T. Sommer, Z. Hadzibabic, T. Yefsah, W. S. Bakr, and M. W. Zwierlein, Phys. Rev. Lett. **109**, 095302 (2012).
[21] C. Nayak, S. H. Simon, A. Stern, M. Freedman, and S. Das Sarma, Rev. Mod. Phys. **80**, 1083 (2008).
[22] D. A. Ivanov, Phys. Rev. Lett. **86**, 268 (2001).
[23] L. Fu and C. L. Kane, Phys. Rev. Lett. **100**, 096407 (2008).
[24] M. Sato, Y. Takahashi, and S. Fujimoto, Phys. Rev. Lett. **103**, 020401 (2009).
[25] C. Zhang, S. Tewari, R. M. Lutchyn, and S. Das Sarma, Phys. Rev. Lett. **101**, 160401 (2008).
[26] J. Liu, Q. Han, L. B. Shao, and Z. D. Wang, Phys. Rev. Lett. **107**, 026405 (2011).
[27] J. Linder, Y. Tanaka, T. Yokoyama, A. Sudbø, and N. Nagaosa, Phys. Rev. Lett. **104**, 067001 (2010).
[28] J. D. Sau, S. Tewari, R. M. Lutchyn, T. D. Stanescu, and S. Das Sarma, Phys. Rev. B **82**, 214509 (2010).
[29] S.-L. Zhu, L.-B. Shao, Z. D. Wang, and L.-M. Duan, Phys. Rev. Lett. **106**, 100404 (2011).
[30] X.-J. Liu, L. Jiang, H. Pu, and H. Hu, Phys. Rev. A **85**, 021603(R) (2012).

[31] L. Jiang, T. Kitagawa, J. Alicea, A. R. Akhmerov, D. Pekker, G. Refael, J. I. Cirac, E. Demler, M. D. Lukin, and P. Zoller, Phys. Rev. Lett. **106**, 115302 (2011).
[32] T. Zhou and Z. D. Wang, Phys. Rev. B **88**, 155114 (2013).
[33] Y. X. Zhao and Z. D. Wang, Phys. Rev. B **90**, 115158 (2014); Y. Hu, Y. X. Zhao, Z.-Y. Xue, and Z. D. Wang, arXiv:1407.6230.
[34] S. Nadj-Perge, I. K. Drozdov, J. Li, H. Chen, S. Jeon, J. Seo, A. H. MacDonald, B. Andrei Bernevig, and A. Yazdani, Science **346**, 602 (2014).
[35] A. V. Balatsky, I. Vekhter, and J.-X. Zhu, Rev. Mod. Phys. **78**, 373 (2006).
[36] J. D. Sau and E. Demler, Phys. Rev. B **88**, 205402 (2013).
[37] X.-J. Liu, Phys. Rev. A **87**, 013622 (2013).
[38] Y. Nagai, Y. Ota, and M. Machida, arXiv:1407.1125.
[39] M. Wimmer, A. R. Akhmerov, M. V. Medvedyeva, J. Tworzydlo, and C. W. J. Beenakker, Phys. Rev. Lett. **105**, 046803 (2010).
[40] H. Hu, L. Jiang, H. Pu, Y. Chen, and X.-J. Liu, Phys. Rev. Lett. **110**, 020401 (2013).
[41] Y. Nagai, Y. Ota, and M. Machida, Phys. Rev. B **89**, 081103(R) (2014).
[42] Y. Nagai, Y. Ota, and M. Machida, J. Phys. Soc. Jpn. **83**, 094722 (2014).
[43] Z. Wang, J. R. Engelbrecht, S. Wang, H. Ding, and S. H. Pan, Phys. Rev. B **65**, 064509 (2002).
[44] J.-H. Chen, C. Jang, S. Adam, M. S. Fuhrer, E. D. Williams, and M. Ishigami, Nat. Phys. **4**, 377 (2008).
[45] For the in-plane charged impurity, the long-range interactions are perfectly screened. An additional screened potential is required to simulate the real system.
[46] T. Zhou, Y. Gao, and Z. D. Wang, Sci. Rep. **4**, 5218 (2014).
[47] L. Fu and C. L. Kane, Phys. Rev Lett. **102**, 216403 (2009).
[48] A. R. Akhmerov, J. Nilsson, and C. W. J. Beenakker, Phys. Rev. Lett. **102**, 216404 (2009).
[49] Y. Tanaka, T. Yokoyama, and N. Nagaosa, Phys. Rev. Lett. **103**, 107002 (2009).
[50] S. B. Chung, X.-L. Qi, J. Maciejko, and S.-C. Zhang, Phys. Rev. B **83**, 100512(R) (2011).
[51] S. Walter, T. L. Schmidt, K. Borkje, and B. Trauzettel, Phys. Rev. B **84**, 224510 (2011).
[52] K. Flensberg, Phys. Rev. Lett. **106**, 090503 (2011).